

A Neutron Small-Angle Scattering Study of Hen Egg-White Lysozyme

BY H. B. STUHRMANN*

Institut für physikalische Chemie der Universität Mainz, D6500 Mainz, Germany (BRD)

AND H. FUESS

Institut Laue-Langevin, BP N° 156, 38042 Grenoble Cedex, France

(Received 3 March 1975; accepted 28 June 1975)

The neutron small-angle scattering of hen egg-white lysozyme chloride in solution has been determined. The scattering density of the solvent and accordingly its contrast with the dissolved particles has been varied by changing the H₂O/D₂O ratio of the solvent. The zero-angle scattering was derived and it was shown that the square root of the zero-angle intensity is proportional to the contrast. The experimental value of the radius of gyration is $R = 13.8 \text{ \AA}$, in good agreement with the same quantity calculated on the basis of the crystal structure model of tetragonal lysozyme. The three basic scattering functions were derived from the experimental data and compared with the corresponding scattering pattern calculated from the coordinates of the X-ray structure. The results do not suggest a deviation of the conformation and structure of lysozyme in solution from the crystal structure. The spherical average of the overall dimensions has been separated from the internal structure. The influence of higher multipoles of the shape of the lysozyme molecule on the scattering curve is discussed.

Introduction

Lysozymes (mucoprotein *N*-acetylmuranylhydrolases) form a class of rather widely distributed enzymes occurring in many tissues and secretions of vertebrates, bacteria, phages and plants (*e.g.* Jollés & Jollés, 1969).

In the following the term lysozyme is used for the specific form hen egg-white lysozyme. The structure of this lysozyme has been determined by Blake, Koenig, Mair, North, Phillips & Sarma (1965) who worked on the tetragonal crystal modification of lysozyme chloride. The structure of a triclinic modification has been reported (Joynson, North, Sarma, Dickerson & Steinrauf, 1970). The conformation of the molecule is the same in the two modifications. Recently a phase transition has been described (Jollés & Berthou, 1972) for tetragonal lysozyme which becomes orthorhombic at temperatures higher than 25°C. This orthorhombic form is called lysozyme B; crystal structure analysis is in progress. It is not yet clear whether the crystal structure transition is accompanied by a transition in the conformation. The question whether the conformation in the crystalline form is identical to lysozyme in solution was, however, not completely solved. Some evidence for the conservation of the molecular structure was given by a comparison of earlier X-ray small-angle scattering experiments (Luzzati, Witz & Nicolaieff, 1961) with the structural model. The results of more recent work of Krigbaum & Kügler (1970) are compatible with the structural model.

The introduction of the contrast variation technique (Stuhrmann & Kirste, 1965) allows more information

to be extracted from small-angle scattering studies in solution. The analysis of the three basic scattering functions provides specific information on the scattering due to the shape of the molecule and to its internal structure (Stuhrmann, 1974).

Contrast variation is easily achieved in neutron scattering experiments. A wide range of scattering-length densities can be covered with H₂O/D₂O mixtures because the scattering length of H ($-0.374 \times 10^{-12} \text{ cm}$) and of D ($+0.667 \times 10^{-12} \text{ cm}$) are very different. As the scattering lengths of the other relevant nuclei in protein molecules do not differ much from that of D (except N with $b = 0.94 \times 10^{-12} \text{ cm}$) the internal structure density function $\rho_s(\mathbf{r})$ is mainly determined by the H density of the protein molecule.

The present paper describes an analysis of the basic scattering functions of dissolved lysozyme in terms of a multipole expansion. The limits of an unambiguous interpretation are presented and the results are compared with the structural model of tetragonal lysozyme chloride.

II. Experimental

The lysozyme was supplied by Koch-Light and labelled lysozyme chloride ex egg white, cryst. (batch N° 55982). Ten different D₂O/H₂O mixtures ranging from pure D₂O to pure H₂O were used as solvent. The aqueous solution had a pH of 3.65 and *p*D for the solution in D₂O was 3.82 (both for 40 mg/ml). Series of decreasing concentration were prepared in pure D₂O and pure H₂O. The weight concentration of lysozyme in the mixtures of H₂O/D₂O was uniformly 80 mg/ml. All scattering curves were extrapolated to infinite dilution of lysozyme in order to eliminate interparticle interference in the small-angle scattering.

* Former research participant of the Institut Laue-Langevin, Grenoble, France.

The neutron scattering experiments were done at the small-angle scattering device D11 at the Institut Laue-Langevin. This instrument is installed at a neutron guide tube at the cold source of the reactor. Neutrons are monochromatized by a helical slit selector and detected by a two-dimensional position sensitive detector of 64×64 counting points arranged in a square of 64 cm height. A detailed description of the facility is given by Schmatz, Springer, Schelten & Ibel (1974). The mean wavelength was 3.5 \AA with a half-width of 1.5 \AA . The scattering curves were corrected for the influence of the wavelength distribution. A sufficiently broad range of scattering angle could be covered by placing the detector at distances of 0.66 m and 2.36 m from the sample. The sample area was 2 cm^2 and the sample volume 0.5 ml. The neutron flux passing through the sample was about $5 \times 10^7 \text{ n sec}^{-1} \text{ cm}^{-2}$. The measuring time for one scattering curve was 10 min and about 500 to 2000 counts were recorded per registering point. Runs on each solvent mixture were made to determine the background from the solvent. The experiments were performed at 23°C .

III. The contrast variation technique

As already stated the experiments were performed in the presence of variable amounts of D_2O . The purpose of adding D_2O to H_2O was to raise the scattering density from negative values below 8% D_2O to values which are higher than the scattering density of organic material. It may be noted that the contrast can vary often not be varied sufficiently in X-ray work.

The influence of the solvent on the scattering pattern of the solute is explained in the following way (Stuhrmann & Kirste, 1965; Hyman & Vaughan, 1967; Harrison, 1969; Stuhrmann 1970a, 1974; Mateu, Tardieu, Luzzati, Aggerbeck & Scanu, 1972). In solutions of macromolecules the scattering of the solute can well be described by the difference of the scattering probability between the solute and the solvent. The influence of the solvent on the excess scattering density $\rho(\mathbf{r})$ is approximated by an expression linear in the contrast \bar{q}

$$\rho(\mathbf{r}) = \bar{q} \rho_c(\mathbf{r}) + \rho_s(\mathbf{r}). \quad (1)$$

\bar{q} is the mean excess scattering density ($\bar{q} = \rho_{\text{protein}} - \rho_{\text{solvent}}$). $\rho_c(\mathbf{r})$ is a function which describes the region that is forbidden to the solvent by solute molecules. Without any penetration of solvent into the molecule (inner solvation) and without any replacement of H by D, $\rho_c(\mathbf{r})$ is 1 inside the molecule boundaries and it vanishes outside. In proteins, however, partial penetration of the solvent to the internal parts of the particle is known to occur as well as a dissociation of protons which, in $\text{H}_2\text{O}/\text{D}_2\text{O}$ mixtures, will be replaced by deuterons. These effects are accounted for by values of $\rho_c(\mathbf{r})$ between 0 and 1. $\rho_s(\mathbf{r})$ gives a description of the structure of the dissolved molecule. A direct measurement of this quantity is obtained if the contrast is zero. In this case zero-angle scattering vanishes, a

fact which allows an easy detection of this quantity and provides a valuable reference point in experimental work. The scattered intensity $I(\kappa)$ corresponding to the scattering density $\rho(\mathbf{r})$ from (1) consists of three basic scattering functions (Stuhrmann & Kirste, 1965):

$$I(\kappa) = \bar{q}^2 I_c(\kappa) + \bar{q} I_{cs}(\kappa) + I_s(\kappa). \quad (2)$$

IV. Results and discussion

1. Zero-angle scattering

The extrapolation of small-angle scattering to $\kappa=0$ yields zero-angle scattering. The square root of the zero-angle intensity of a dilute monodisperse solution is proportional to the contrast \bar{q} . The results of lysozyme in Fig. 1 confirm the linear dependence of $\sqrt{I(0)}$ on the scattering density of the solvent.

The mean scattering density of the solute is given by the intercept of the straight line in Fig. 1 with the abscissa. Zero-angle scattering of lysozyme vanishes at 45% D_2O content in the $\text{H}_2\text{O}/\text{D}_2\text{O}$ mixture. The scattering density of lysozyme is then equal to that of the solvent. The sum of the coherent scattering density of this particular H_2O mixture is $2.55 \times 10^{10} \text{ cm/cm}^3$. The sum of the coherent scattering lengths of the lysozyme molecule can be calculated from the known amino acid sequence. By admitting an exchange of H atoms corresponding to 45% D_2O the total scattering length of $4.50 \times 10^{-10} \text{ cm}$ is obtained. The volume of the lysozyme molecule is given as the ratio of these two quantities $V = (4.50 \times 10^{-10} / 2.55 \times 10^{10}) \text{ cm}^3 = 17800 \text{ \AA}^3$.

2. The radius of gyration

The radius of gyration R^2 is shown in Fig. 2 as a function of the contrast \bar{q} . Fig. 2 suggests a dependence of R^2 on $1/\bar{q}$ which shows only small deviations from linearity

$$R^2 = R_c^2 + \frac{\alpha}{\bar{q}} - \frac{\beta}{\bar{q}^2}. \quad (3)$$

The coefficients α and β are defined by

$$\alpha = \frac{1}{V_c} \int \rho_s(\mathbf{r}) r^2 d^3r$$

$$\beta = \frac{1}{V_c^2} \iint \rho_s(\mathbf{r}) \rho_s(\mathbf{r}') \mathbf{r} \cdot \mathbf{r}' d^3r d^3r'. \quad (4)$$

As already stated $\rho_c(\mathbf{r})$ becomes predominant for high contrast \bar{q} and the radius of gyration then equals R_c [see (3) for $1/\bar{q}$ tending to 0]. The interpolation of the experimental data in Fig. 2 yields $R_c = 13.8 \text{ \AA}$. This radius R_c corresponds to the volume actually occupied by the molecule in solution, because details of the internal structure cease to contribute significantly to $I(\kappa)$ when the contrast tends to infinity. The same parameter was calculated from the coordinates of the structural lysozyme model for the scattering function $\rho_c(\mathbf{r})$. Unit scattering lengths were assumed for all atoms except the exchangeable H atoms for which $b=0$ was

assumed. According to the estimation of static accessibility of solvent molecules to lysozyme by Lee & Richards (1971) the penetration of the internal region by water molecules could be neglected. The numerical value of $R_c = 13.85 \text{ \AA}$ was obtained which compares remarkably well with the experimental value.

In an $\text{H}_2\text{O}/\text{D}_2\text{O}$ mixture containing 8% D_2O the coherent scattering density of the solvent vanishes. The

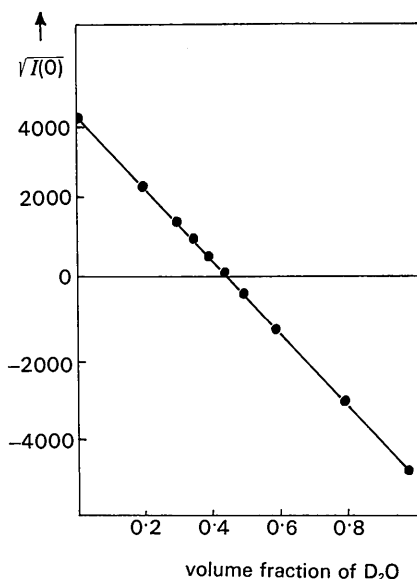


Fig. 1. The square root of zero-angle scattering is a linear function of the volume fraction of D_2O of the solvent. The scale of the ordinate is given in fermi ($= 10^{-13} \text{ cm}$).

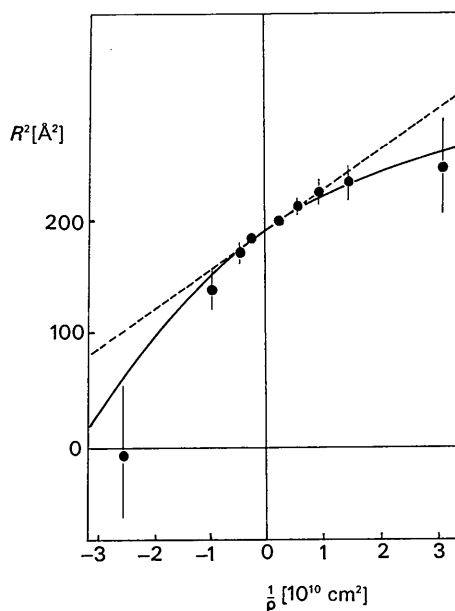


Fig. 2. The square of the radius of gyration R as a function of the reciprocal of the contrast $\bar{\rho}$. The dots with error bars represent experimental results.

scattering pattern of lysozyme as *in vacuo* is observed, if layers of ordered water molecules surrounding the lysozyme molecule are neglected. The radius of gyration of the scattering density of lysozyme in this particular solvent is $R = 14.2 \text{ \AA}$. The value calculated from the atomic coordinates of tetragonal lysozyme (Phillips, 1972) from the actual values of the scattering lengths is 14.05 \AA .

The slope of the tangent (dashed line in Fig. 2) indicates $\alpha = 3.5 \times 10^{-5}$ a value which is found in other solutions of globular proteins (Stuhrmann, 1974) and seems to reflect a common feature of many proteins. An outer region of higher scattering density due to polar groups surrounding a hydrophobic core that is somewhat richer in protons would explain the positive sign of α . From the curvature of the bent line in Fig. 2, β is found to be $4 \times 10^{-12} \text{ \AA}^{-2}$. As β is proportional to $\sum_{m=-1}^1 \left| \int \rho_{1m}(r) r^3 dr \right|^2$ [see equation (9)], the asymmetry of the lysozyme molecule is obvious. The equivalent statement would be that the centre of $\rho(r)$ changes with variable contrast. For $\bar{\rho} = 1 \times 10^{10} \text{ cm}^{-2}$ the displacement amounts to about 2 \AA .

3. The basic scattering functions

From all the scattering curves that of lysozyme *in vacuo* (vanishing scattering density of the solvent for a 8% content of D_2O in H_2O) is most easily compared with a scattering function calculated from the lysozyme structure coordinates

$$I(\kappa) = \sum_i \sum_j b_i b_j \frac{\sin \kappa |\mathbf{r}_i - \mathbf{r}_j|}{\kappa |\mathbf{r}_i - \mathbf{r}_j|}. \quad (5)$$

The structural coordinates of all non-hydrogen atoms have been determined by X-ray diffraction (Phillips, 1972). The positions of the H atoms were generated from the coordinates of the heavy atoms by means of a PL1 program which had already been tested with other protein structure data (Stuhrmann, 1973). For $\kappa > 0.5 \text{ \AA}^{-1}$ the calculated scattering curve $I(\kappa)$ agrees with the experimental results (Fig. 3). The analysis of small-angle scattering in terms of multipoles can be very fruitful, especially if we are interested in the origin of certain details of the scattering curve. Furthermore it leads to a clearer understanding of the basic scattering functions. The mathematical background which has already been reported (Harrison, 1969; Stuhrmann 1970a) will be briefly outlined.

The scattering density function $\rho(\mathbf{r})$ is expanded in a series of spherical harmonics $Y_{lm}(\omega)$, ω being a unit vector with components θ and φ , the polar angles;

$$\rho(\mathbf{r}) = \sum_{l=0}^{\infty} \sum_{m=-l}^l \rho_{lm}(r) Y_{lm}(\omega). \quad (6)$$

Due to the completeness of the spherical harmonics any arbitrary $\rho(\mathbf{r})$ can be described by an appropriate choice of the radial function $\rho_{lm}(r)$. From the orthog-

onality of the spherical harmonics $Y_{lm}(\omega)$ it follows that

$$\varrho_{lm}(r) = \int \varrho(\mathbf{r}) Y_{lm}^*(\omega) d\omega. \quad (7)$$

The scattering function of dissolved particles is in this formalism given by

$$I(\kappa) = 2\pi^2 \sum_{l=0}^{\infty} \sum_{m=-l}^l |A_{lm}(\kappa)|^2 \quad (8)$$

with

$$A_{lm}(\kappa) = \sqrt{\frac{2}{\pi}} i^l \int_0^{\infty} \varrho_{lm}(r) j_l(\kappa r) r^2 dr,$$

where $j_l(\kappa r)$ are the spherical Bessel functions of order l .

$A_{lm}(\kappa)$ is a multipole component of the geometrical structure factor of $\varrho(\mathbf{r})$. The scattering intensity $I(\kappa)$ was calculated for $l=0, 2, 4, 6$ and 10 as the highest values of the multipole expansion. These curves are shown in Fig. 3 with the experimental curve. The termination index $l=\infty$ is defined by (5). The conservation of $I(\kappa)$ on rotation of $\varrho(\mathbf{r})$ is expressed by the fact that it has the form of a scalar product in the space of spherical harmonics

$$I = \langle A|A \rangle. \quad (9)$$

The relations between the basic scattering functions are clarified by combining (9) and (1)

$$I = \langle \bar{\varrho} A_c + A_s | \bar{\varrho} A_c + A_s \rangle = \bar{\varrho}^2 \langle A_c | A_c \rangle + \bar{\varrho} \langle A_c | A_s \rangle + \langle A_s | A_c \rangle + \langle A_s | A_s \rangle. \quad (10)$$

At a given κ the small-angle scattering data of lysozyme in different $\text{H}_2\text{O}/\text{D}_2\text{O}$ mixtures are approximated by (2).

The resulting basic scattering functions are shown in Figs. 4-6. $I_c(\kappa)$ is represented in the form of its square root. The experimental results agree with scattering curves calculated from the crystal structure. The decrease of accuracy of the experimental data with lower intensity obscures the details especially of $I_s(\kappa)$.

Equation (7) offers an infinite number of possible superpositions of the multipole components without changing $I(\kappa)$ (Stuhrmann, 1970b). The question whether a unique solution out of this infinite number can be found is treated in the next section.

3.1 The spherically averaged structure

How could we find the structure $\varrho(\mathbf{r})$ of the lysozyme molecule if we had only neutron small-angle scattering data? A useful approach to find a unique solution and hence the structure consists in searching for the spherically averaged structure $\langle \varrho(\mathbf{r}) \rangle_{\text{av}} = \varrho_{00}(r)/\sqrt{4\pi}$ which is possible if the particle exhibits almost spherical symmetry (Mateu *et al.*, 1972). In general, spherical symmetry cannot be assumed to be the dominant feature of $\varrho(\mathbf{r})$ and therefore the strategy has to be slightly

modified. A glance at the multipole contributions of the basic scattering functions reveals an interesting fact: The cross-term $I_{cs}(\kappa)$ is dominated by $l=0$ (*i.e.*

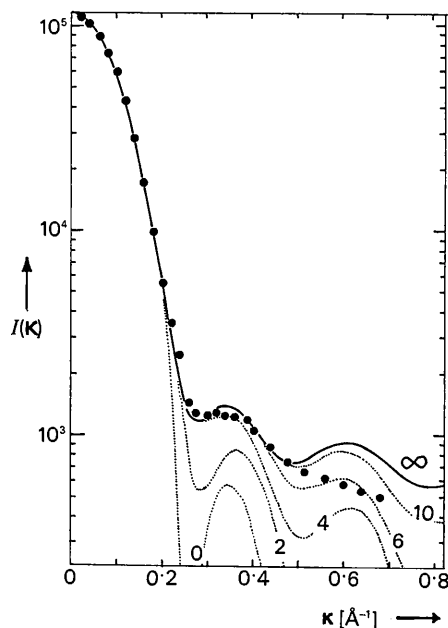


Fig. 3. Neutron scattering of lysozyme *in vacuo* (solvent: $\text{D}_2\text{O}/\text{H}_2\text{O} = \frac{1}{2}$). ● experimental result, — calculated from the model [equation (5)], ··· calculated from the model [equation (8)], with various termination indices]. The scale of the ordinate is given in barns (10^{-24} cm^2).

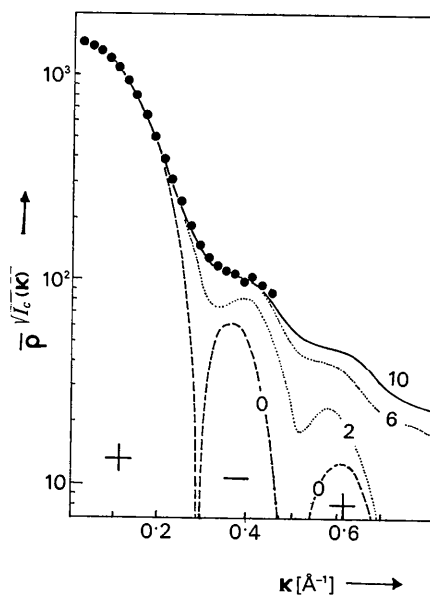


Fig. 4. The square root of $I_c(\kappa)$, with the multipole analysis of $I_c(\kappa)$ as calculated from the model (●) from experimental neutron scattering curves of lysozyme in various $\text{H}_2\text{O}/\text{D}_2\text{O}$ mixtures. The termination indices are given in the figure. The sequence of signs of the spherically averaged amplitude ($l=0$) is alternating. The ordinate is the same as in Fig. 1. $\bar{\varrho} = 10^{-10} \text{ cm}$.

spherical symmetry) up to considerably higher κ than $I_c(\kappa)$ (see Fig. 5). This is not surprising because the absolute squares of the multipoles are always positive whereas the mixed terms of $I_{cs}(\kappa)$ can have negative and positive contributions which cancel each other more and more with increasing l ; i.e. the detailed features of $\varrho_c(\mathbf{r})$ and $\varrho_s(\mathbf{r})$ are practically uncorrelated [see equation (11)]. For values of κ which are not too large the basic scattering functions are

$$I_c(\kappa)/2\pi^2 = [A_{00}^c(\kappa)]^2 + \sum_{m=-1}^1 |A_{2m}^c(\kappa)|^2 + \sum_{m=-2}^2 |A_{4m}^c(\kappa)|^2$$

$$I_{cs}(\kappa)/4\pi^2 = A_{00}^c(\kappa) \cdot A_{00}^s(\kappa) \quad (11)$$

$$I_s(\kappa)/2\pi^2 = [A_{00}^s(\kappa)]^2 + \sum_{m=-1}^1 |A_{1m}^s(\kappa)|^2 + \dots$$

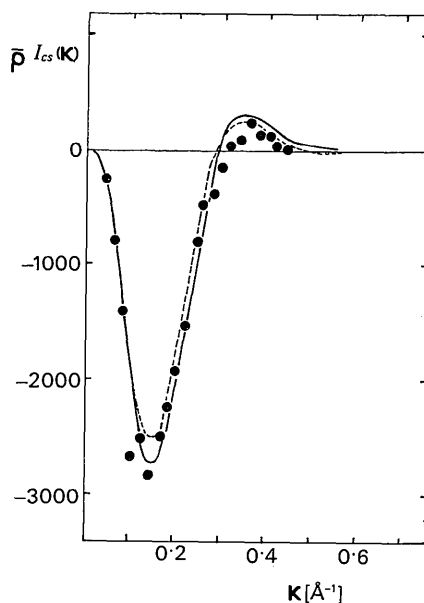


Fig. 5. The mixed scattering function $I_{cs}(\kappa)$ of lysozyme. ● experimental results, --- calculated from the model with equation (8), termination index $l=0$, — calculated from the model with equation (8), termination index $l \geq 4$. Ordinate as in Fig. 1.

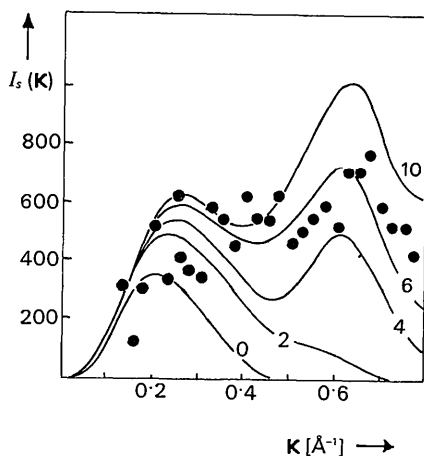


Fig. 6. Neutron scattering of lysozyme at vanishing contrast. ● experimental results. The full lines represent scattering curves, which are calculated from the model with equation (8). The termination indices are shown in the figure. Ordinate as in Fig. 3.

The dipole contribution ($l=1$) in $I_c(\kappa)$ might be rather small because the centre $\varrho_c(\mathbf{r})$ is at the origin. Its power series in κ^2 starts only with κ^4 , as does the quadrupole term ($l=2$). The latter describes the anisotropy of the molecular dimensions and is more important even if the molecular structure exhibits considerable asymmetry, which is due to odd l . The presence of the dipole term in $I_s(\kappa)$ on the other hand has already been shown during the analysis of the radius of gyration. β^2 is the first coefficient of its power series which starts with κ^2 .

The spherically averaged amplitudes were estimated in the following manner: at small κ $A_{00}^c(\kappa)$ is practically equal to $\sqrt{I_c(\kappa)}$ and it is positive as $\varrho_c(\mathbf{r})$ is always positive. As $I_{cs}(\kappa)$ is negative $A_{00}^s(\kappa)$ must equally be negative in this κ region in agreement with the positive value of α . At $\kappa = 0.29 \text{ \AA}^{-1}$ the function $I_{cs}(\kappa)$ passes through zero (see Fig. 5). Either $A_{00}^s(\kappa)$ or $A_{00}^c(\kappa)$ are changing sign. Inspection of Fig. 4 leaves no doubt that $A_{00}^c(\kappa)$ is vanishing at this particular value of κ .

In order to calculate numerically any radial function it is approximated by an analytical expression. These calculations are then compared with those based on the lysozyme X-ray structure. For this purpose the Laguerre polynomials $L_n^a(x^2)$ are very convenient because the Hankel transformation is simply achieved by changing the sign of the polynomials with odd n :

$$\int \frac{2}{\pi} \int_0^\infty \exp(-x^2/2) L_n^{l+1/2}(x^2) J_l(xy) x^2 dx$$

$$= (-1)^n y^l \exp(-y^2/2) L_n^{l+1/2}(y^2). \quad (12)$$

Two conditions define $A_c(\kappa)_{av}$: $A_c(0) = 1450$ (see Fig. 4) and $A_c(\kappa)_{av} = 0$ at $\kappa = 0.29 \text{ \AA}^{-1}$ (Fig. 7). Two coefficients of the series are determined

$$f(x) = c_0 L_0^{1/2}(x^2) + c_1 L_1^{1/2}(x^2) = c_0 \exp(-x^2/2)$$

$$+ c_1 \left(\frac{3}{2} + x^2\right) \exp(-x^2/2). \quad (13)$$

The quality of this approximation is strongly influenced by the transformation of the abscissa. At small κ the Guinier approximation holds:

$$\sqrt{I(\kappa)} = A_c(\kappa) = \bar{\varrho} V_c (1 - \frac{1}{6} R_c^2 \kappa^2 + \dots). \quad (14)$$

With the transformation factor $(R/\sqrt{6})/(1/\sqrt{2}) = R/\sqrt{3} = 8$ the following numerical values were obtained (Figs. 7, 8):

$$A_{00}^c(x) = 1030 + 280 \left(\frac{3}{2} - x^2\right) \exp(-x^2/2)$$

$$\varrho_{00}^c(x) = 1030 - 280 \left(\frac{3}{2} - x^2\right) \exp(-x/2). \quad (15)$$

The spherically averaged internal structure $\langle \rho_s(\mathbf{r}) \rangle$ was calculated in a similar way (Figs. 7, 8):

$$\begin{aligned} A_{00}^s(x) &= -300 + 200\left(\frac{3}{2} - x^2\right) \exp(-x^2/2) \\ &= -300x^2 \exp(-x^2/2) \\ \rho_{00}^s(x) &= -300 - 200\left(\frac{3}{2} - x^2\right) \exp(-x^2/2). \end{aligned} \quad (16)$$

Here it was taken into account that $A_s(0) = 0$ and at small κ the relation $\langle A_s(\kappa) \rangle = I_{cs}(\kappa)/2 \langle A_c(\kappa) \rangle$ holds. A remarkably good approximation of the radial scattering density of the lysozyme model has been achieved for both the internal structure and the overall dimensions.

The approximations which are described above give better agreement with the experimental curves than does a simple Gaussian fit (Figs. 7, 8).

As we did not make any absolute measurements we should explain how an absolute scaling of Fig. 8 has been achieved. For the scale of the ordinate the influence of H/D exchange has to be considered. The mean value of $\rho_c(\mathbf{r})$ is 0.8. On the basis of a decreased density of polar groups in the central part (Lee & Richards, 1971) $\rho_c(0) = 0.9$ has been assumed.

3.2 Higher multipole components

From the rather slow decrease of $\langle \rho_c(\mathbf{r}) \rangle$ between $r = 10$ and 23 \AA (Fig. 8) it is concluded that this region is partially accessible to the solvent whereas the core appears to be relatively homogeneous at a resolution of 15 \AA . The possibility that the outer region is made up of loosely padded segments of the protein chain, which would result in a spherical structure, can be excluded, because the rather considerable difference between the square root of $I(\kappa)$ and $A_c(\kappa)$ at $\kappa < 0.2$ (Fig. 7) betrays the presence of multipole components with low index l .

The difference between $I_c(\kappa)$ and $|\langle A_c(\kappa) \rangle|^2$ seems to start with κ^2 (broken line in Fig. 9). A dipole structure $\rho_1(\mathbf{x}) = x \exp(-0.5 \cdot x^2) \cos \theta$ would give rise to a scattering pattern $I_1(x) = x^2 \exp(-x^2)$. After subtracting an appropriate amount of $I_1(x)$ (dotted line in Fig. 9) from the first difference, we are left with a residue which starts with κ^4 . This second difference can be interpreted in terms of a quadrupole structure $\rho_2(\mathbf{r})$

$$\rho_2(\mathbf{r}) = \sum_{m=-2}^2 \rho_{2m}(r) Y_{2m}(\theta, \varphi). \quad (17)$$

The choice of the sign and the index of the coefficients is arbitrary, because the sum of the absolute squares of $A_{2m}(\kappa)$ enters into the interpretation. Prolate or oblate partial structures would result, depending on whether the positive or negative sign is preferred. The spatial orientation of the main axes of the quadrupole is governed by the weight of the $\rho_{2m}(r)$. Fig. 9 shows the superposition of $\rho_0(r) + \rho_1(r)$ and $\rho_0(r) + \rho_2(r)$. Both partial structures have rotational symmetry [which is already an arbitrary restriction for $\rho_2(r)$]. Any superposition of the independently rotated structures $\rho_0(r)$, $\rho_1(r)$, and $\rho_2(r)$ is a possible structure which fits the

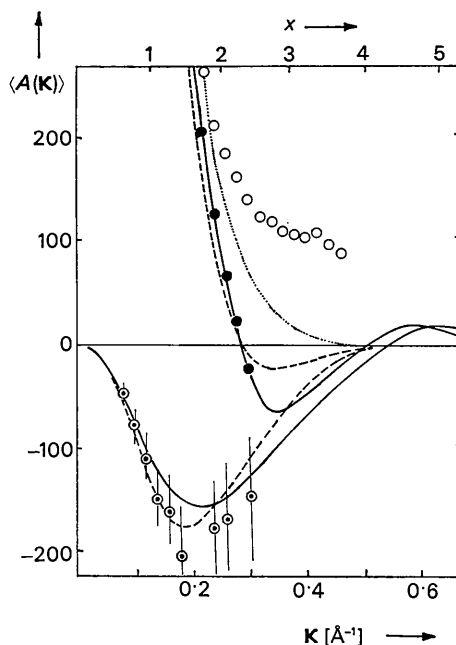


Fig. 7. The averaged amplitudes $\langle A(\kappa) \rangle$ of the overall dimension $\langle A_c(\kappa) \rangle$. ● graphical estimation, taking into account good approximation of $I(\kappa)$ in the Guinier zone and the zero at $\kappa = 0.29 \text{ \AA}^{-1}$. — calculated from the lysozyme model. ··· approximation by a Gaussian curve [$= L_0^{1/2}(x^2)$]. --- approximation by $L_0^{1/2}(x^2)$ and $L_1^{1/2}(x^2)$. The averaged amplitude of the internal structure $A_s(\kappa)$ (lower part): ● $I_{cs}(\kappa)/2 \langle A_c(\kappa) \rangle = \langle A_s(\kappa) \rangle$. --- approximation by $L_0^{1/2}(x^2)$ and $L_1^{1/2}(x^2)$. The ordinate is the same as in Fig. 1. All Laguerre polynomials L are weighted by $\exp(-x^2/2)$. ○ root of $I_c(\kappa)$.

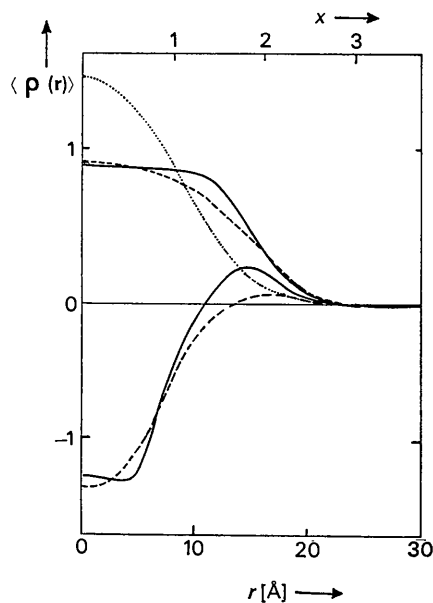


Fig. 8. The radial scattering density distributions of the overall structure $\langle \rho_c(r) \rangle$ (upper part of the figure) and the internal structure $\rho_s(r)$ (lower part of the figure). — calculated from the model, ··· approximation by a Gaussian [only for $\rho_c(r)$]. --- approximation by $L_0^{1/2}(x^2)$ and $L_1^{1/2}(x^2)$. The units of the ordinate are 10^{10} cm^{-2} .

scattering curve $I_c(\kappa)$ equally well (Stuhrmann, 1970b). Structures resembling a pear may result as well as shapes like beans depending on the mutual orientation of $\varrho_1(\mathbf{r})$ and $\varrho_2(\mathbf{r})$. From crystallographic studies (Blake *et al.*, 1965) it is known that the shape of the lysozyme

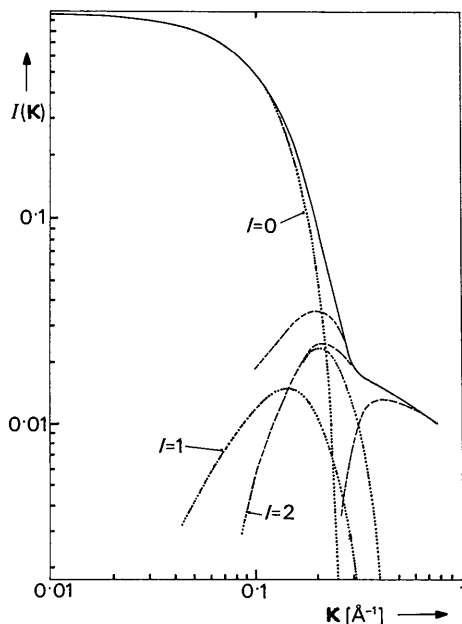


Fig. 9. The scattering curve $I_c(\kappa)$ analysed in terms of partial scattering functions (\cdots), which originate from various multipole components of $\varrho_c(\mathbf{r})$. — $I_c(\kappa)$. The differences resulting from the subtraction of a partial scattering function are shown by broken lines (---).

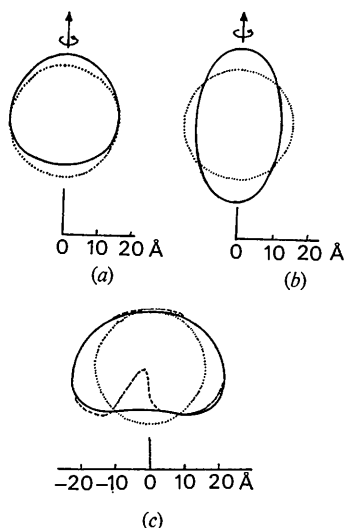


Fig. 10. The partial structures of the lysozyme molecule. The contour lines represent half the maximum value of $\varrho_c(\mathbf{r})$. \cdots $\varrho_0(\mathbf{r})$ (a) — $\varrho_0(\mathbf{r}) + \varrho_1(\mathbf{r})$. (b) — $\varrho_0(\mathbf{r}) + \varrho_2(\mathbf{r})$. (c) — $\varrho_0(\mathbf{r}) + \varrho_1(\mathbf{r}) + \varrho_2(\mathbf{r})$. --- a cross section of the lysozyme model showing the cleft with its active site (Phillips, 1972).

molecule is concave. A bean-like structure (the quadrupole term in Fig. 10 is turned by $\pi/2$) fits the known lysozyme model fairly well. The cleft of the lysozyme molecule with its active site is not clearly resolved by this method (Fig. 10). If small-angle scattering functions are treated according to this general method a unique solution for the structure cannot be given but the whole family of possible structures can be derived from the scattering curve. The only restriction that $\varrho_c(\mathbf{r})$ is always positive is useful to eliminate a part of the solutions. This restriction is in the case of lysozyme not sufficient to obtain a unique solution. If $\varrho_c(\mathbf{r})$ is constant everywhere inside the lysozyme molecule, the correlation between the multipoles would be much stronger and a unique structure determination seems to be possible at least at low resolution (Stuhrmann, 1970a). This, however, would only be the case for solvents having no interaction with lysozyme. The experimental scattering curve $\varrho_c(\mathbf{r})$ of lysozyme in $\text{H}_2\text{O}/\text{D}_2\text{O}$ mixtures does not fulfil this condition, but it is close to one in hydrophobic regions and rather low in regions of the molecule with polar groups and dissociating protons. A structure determination from $I_c(\kappa)$ is therefore prohibitively difficult. Higher multipole components of the internal structure cannot be calculated because the experimental $I_s(\kappa)$ are too inaccurate (Fig. 6).

Conclusions

Although we restricted the interpretation of the experimental results to rather low momentum transfer κ , some features of the lysozyme molecule, which seem to be typical for globular proteins, have been revealed by the contrast variation method. Neutron scattering proves to be especially suitable for the application of the solvent exchange technique. Owing to the higher quality of data new limits of structure determination by small-angle scattering could be defined.

The authors are indebted to Dr K. Ibel for assisting with the neutron scattering experiments and to Dr S. A. Mason for reading the manuscript. They thank the former directors of the Institute Laue-Langevin, Professor H. Maier-Leibnitz and Dr B. Jacrot, for their interest in the work. One of them (HBS) wishes to express his gratitude to the directors and colleagues of ILL for their hospitality during his affiliation with the Institute.

References

- BLAKE, C. C. F., KOENIG, D. F., MAIR, G. A., NORTH, A. C. T., PHILLIPS, D. C. & SARMA, V. R. (1965). *Nature, Lond.* **206**, 757-761.
 HARRISON, S. C. (1969). *J. Mol. Biol.* **42**, 457-483.
 HYMAN, A. & VAUGHAN, P. A. (1967). *Small Angle X-ray Scattering*, Edited by H. BRUMBERGER, p. 477. New York: Gordon and Beach.
 JOLLÉS, P. & BERTHOU, J. (1972). *FEBS Lett.* **23**, 21-23.

- JOLLÉS, J. & JOLLÉS, P. (1969). *Helv. Chim. Acta*, **52**, 2671–2675.
- JOYNSON, M. A., NORTH, A. C. T., SARMA, V. R., DICKERSON, R. E. & STEINRAUF, L. K. (1970). *J. Mol. Biol.* **50**, 137–142.
- KRIGBAUM, W. R. & KÜGLER, F. R. (1970). *Biochemistry*, **9**, 1216–1223.
- LEE, B. & RICHARDS, F. M. (1971). *J. Mol. Biol.* **55**, 379–400.
- LUZZATI, V., WITZ, J. & NICOLAIEFF, A. (1961). *J. Mol. Biol.* **3**, 367–378.
- MATEU, L., TARDIEU, A., LUZZATI, V., AGGERBECK, L. & SCANU, M. (1972). *J. Mol. Biol.* **70**, 105–116.
- PHILLIPS, D. C. (1972). Personal communication.
- SCHMATZ, W., SPRINGER, T., SCHELLEN, J. & IBEL, K. (1974). *J. Appl. Cryst.* **7**, 96–116.
- STUHRMANN, H. B. (1970a). *Z. phys. Chem.* **72**, 185–198.
- STUHRMANN, H. B. (1970b). *Acta Cryst.* **A26**, 297–306.
- STUHRMANN, H. B. (1973). *J. Mol. Biol.* **77**, 363–369.
- STUHRMANN, H. B. (1974). *J. Appl. Cryst.* **7**, 173–178.
- STUHRMANN, H. B. & KIRSTE, R. G. (1965). *Z. phys. Chem.* **46**, 247–250.

Acta Cryst. (1976). **A32**, 74

An Improved Probabilistic Theory in $P\bar{1}$ of the Invariant $E_{\mathbf{h}}E_{\mathbf{k}}E_{\mathbf{l}}E_{\mathbf{h}+\mathbf{k}+\mathbf{l}}$

BY C. GIACOVAZZO

Istituto di Mineralogia e Petrografia, Università degli Studi di Bari, Italy

(Received 28 May 1975; accepted 12 June 1975)

The probabilistic approach used by the author in a preceding paper [*Acta Cryst.* **A31**, 252–259] for deriving the sign of quartet relations is used to obtain formulae which take terms of order $1/N^2$ into account. Experimental tests show that the overall reliability of the quartets is better estimated by these formulae, but does not reach the reliability of the triplets. Probabilistic formulae are then rescaled by suitable empirical factors. The new expressions lead to an improvement compared both with theoretical formulae and with the empirical [Schenk (1975). *Acta Cryst.* **A31**, 259–263] method: what is more significant, the new quartets are almost always found to be more reliable than triplets.

Introduction

Recently several papers have been devoted to the estimate of the cosine invariant

$$\cos(\varphi_{\mathbf{h}} + \varphi_{\mathbf{k}} + \varphi_{\mathbf{l}} - \varphi_{\mathbf{h}+\mathbf{k}+\mathbf{l}}).$$

Schenk (1973a) compared the reliability of the relation

$$\varphi_{\mathbf{h}} + \varphi_{\mathbf{k}} + \varphi_{\mathbf{l}} - \varphi_{\mathbf{h}+\mathbf{k}+\mathbf{l}} = 0$$

as a function of

$$E_4 = N^{-1} |E_{\mathbf{h}}E_{\mathbf{k}}E_{\mathbf{l}}E_{\mathbf{h}+\mathbf{k}+\mathbf{l}}| \times \left\{ 1 + \frac{E_{\mathbf{h}+\mathbf{k}} + E_{\mathbf{h}+\mathbf{l}} + E_{\mathbf{k}+\mathbf{l}}}{E_{000}} \right\}, \quad (1)$$

with that of the \sum_2 relationship as a function of

$$E_3 = |E_{\mathbf{h}}E_{\mathbf{k}}E_{\mathbf{l}}|/\sqrt{N}.$$

From a probabilistic point of view Hauptman (1974a) derived a negative cosine invariant expression, subject to the condition $|E_{\mathbf{h}+\mathbf{k}}| \simeq |E_{\mathbf{h}+\mathbf{l}}| \simeq |E_{\mathbf{k}+\mathbf{l}}| \simeq 0$:

$$\cos(\varphi_{\mathbf{h}} + \varphi_{\mathbf{k}} + \varphi_{\mathbf{l}} - \varphi_{\mathbf{h}+\mathbf{k}+\mathbf{l}}) = -\frac{I_1(B)}{I_0(B)},$$

where $B = 2|E_{\mathbf{h}}E_{\mathbf{k}}E_{\mathbf{l}}E_{\mathbf{h}+\mathbf{k}+\mathbf{l}}|/N$ and I_1 and I_0 are the modified Bessel functions of order one and zero.

Schenk & de Jong (1973) and Schenk (1973b, 1974) proved from semi-empirical observations that negative quartets and quartets of the special type ($\mathbf{h} = \mathbf{k}$) are very useful in finding the correct solution from a set of \sum_2 solutions in symmorphic space groups. A probabilistic theory of these special quartets in $P1$ and $P\bar{1}$ was given by Giacobazzo (1974a, b).

Hauptman (1974b) gave in $P1$ a probabilistic theory of the general cosine invariant $\cos(\varphi_{\mathbf{h}} + \varphi_{\mathbf{k}} + \varphi_{\mathbf{l}} - \varphi_{\mathbf{h}+\mathbf{k}+\mathbf{l}})$ subject to no restrictive conditions. This theory leads to an estimate for the value of the cosine which may lie anywhere between -1 and $+1$.

Independently and by a different mathematical approach Giacobazzo (1975a) derived in $P\bar{1}$ probabilistic expressions for quartets which can in principle replace former formulations. The reliability of the chief formulae derived in this paper was explored by Schenk (1975) who proved that the new expressions:

(a) lead to an improvement compared with the empirical estimate of the reliability of the negative quartets (Schenk, 1974)

(b) over-estimate the probability of the strongly defined positive quartets.

The aim of this paper is to improve the theoretical results previously described (Giacobazzo, 1975a, referred to as paper I) from two points of view: